Department of Wood Engineering

University of West-Hungary

Sopron

Progress Report

No.3.

INSIGHT INTO THE MECHANISM OF WOOD SANDING

Magoss Endre

Sopron

2015

INSIGHT INTO THE MECHANISM OF WOOD SANDING

Progress Report No.3

Published in 2015 by the Department of Wood Engineering
University of West Hungary Sopron
Printed in Sopron, Hungary
by LŐVÉR-PRINT NYOMDAIPARI KFT
2015

ISSN 2060-3649
ISBN 978-963-359-062-1

INSIGHT INTO THE MECHANISM OF WOOD SANDING

Contents

Abstract

Abrasive sanding is one of the most important operations to achieve high quality surfaces in the wood industry. The sanding is an unusual cutting process due to its spherical cutting edge with negative rake angle and random position of grits to each other. Using the laws of engineering mechanics, a detailed analysis was undertaken to clear the various distinct effect of cutting edges. The negative rake angle of the cutting edge is inclined to compress the upper layer of the surface which can be detrimental concerning surface stability. Experiments have shown that especially the thickness of the core depth R_k is very sensitive on deformations caused by the cutting edge.

An interesting comparison was made between the action of tool edges as a cylindrical body and the spherical edge (grit) on the underlying layers concerning their stress fields as a function of depth. This analysis helped to find an equivalence of edge radii for tools and grits concerning their compaction and crushing effects. Experimental results support the theoretical findings.

Based on a detailed experimental work, the general regularities of the sanding process are given for quite different wood species.

The experimental result are presented in diagrams showing the basic relationships between the surface roughness parameters and grit diameters, the roughness parameters and structure number for all wood species, and internal relationship between roughness parameters.

Introduction

The abrasive sanding is one of the most important woodworking operations to produce high quality wood products. Due to the unusual cutting edge with negative rake angle and random position of grits on the surface, the sanding process is very complicated phenomenon hardly allowing an accurate mathematical description. Nevertheless, using the general laws of contact mechanics some general rules could have been derived [1].

Several research works have been done to determine the surface roughness at sanding for different wood species and operational parameters [2, 3, 4]. Earlier experiments have shown that the grit size the radius of edges has a distinct effect on the core depth of the material ratio curve (R_k) [2, 5]. Furthermore, the determination of a minimum roughness due to the internal (anatomical) structure of wood [6] revealed that a clogging phenomenon should take place at sanding producing better roughness than the theoretically possible one. Therefor a detailed investigation program was undertaken to clear the different effects of wood species and operational parameters on the wood surface roughness at sanding.

The various sanding operations are one of the most important woodworking processes to achieve smooth and even surface ensuring high quality in the product manufacture. The sanding is a special cutting process in which material is removed by an unusual cutting edge with negative rake angle (Figure 1).

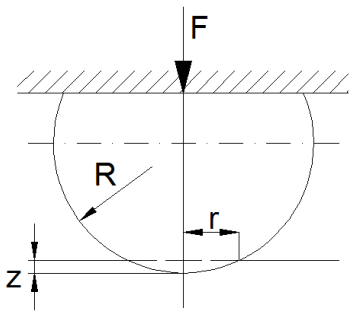

Figure 1 Deformation under a spherical grit

The cutting edge is more or less a hard sphere with a radius *R* embedded in a carrying material (sand paper). The chip formation and the removed material depends on the compression yield stress of the wood, the vertical load on the cutting edge (surface pressure), the radius of the cutting sphere (grit size) and on the cutting velocity.

The grit size is determined by the number of meshes per inch of the sieves used for screening. The real size of the grits is generally taken as normal distributed between two successive sieves. In practice, the average grit size diameter is used as given in Figure 2 as a function of standard grit size notation.

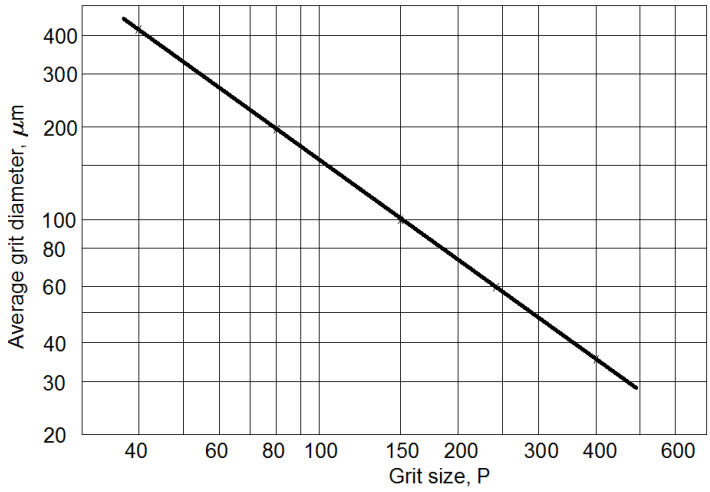

Figure 2. Average grit diameter as a function of standard grit size

The grits are embedded in the base carrying material in a very great numbers and, therefore, they overlap each other many times in their path way. The most important operational parameters are the surface pressure, the feed speed, the grit size and the cutting speed. Beside of these factors, several other influencing parameters may be mentioned such as the hardness of the abrasive material, its heat conduction coefficient, the contact lengths of the sanding etc.

Due to the special shape of the cutting edge and random position of grits embedded in the holding tissue, an accurate description of the sanding process is hardly possible. At the same time, some general relationships and useful approximations can be derived.

In all woodworking operations the spherical edge of the knife exerts a stress field in the underlying material causing distortions and ruptures. This stress field may influence the resultant surface roughness considerably depending on the edge geometry and material properties. The negative rake angle of the cutting edge is inclined to compress the upper layer of the surface which can be detrimental concerning surface stability.

The surface roughness has three characteristic components which are the reduced peak heights R_{pk}, the core depth R_k and the reduced valley depth R_{vk}. Experiments have shown that especially the R_k-layer thickness is very sensitive on deformations caused by the cutting edge.

The resultant R_k-layer thickness may be explained by the combined effect of vertical and horizontal loading stresses acting just under the working edges (grit elements, knife edge). An interesting problem is the comparison of the effect of a grit element and a knife edge on the deformation of wood structure just under the sliding edges. This deformation (crushing effect) has probably a definite correlation with the thickness of the R_k-layer. Based on the engineering mechanics, the knife edge is a cylindrical body contacting the infinite half space. A grit element is more or less a spherical body contacting the same half space. This classical mechanical problem was solved by Boussinesq in 1885.

The contact between a cylinder and a plane can be calculated according the Boussinesq in the following manner. The half contact width is

$$b = \sqrt{\frac{4P' \cdot (1-\upsilon)^2 \cdot R}{\pi \cdot E}} = 1.06 \cdot \sqrt{\frac{P' \cdot R}{E}} \qquad (1)$$

The maximum deformation is given by

$$z = 0.567 \cdot \frac{P'}{E}$$

The maximum pressure in the centre line is

$$\sigma_0 = 0.6 \cdot \sqrt{\frac{P' \cdot E}{R}} \qquad \text{and} \qquad \frac{z}{b} = 0.88 \cdot \frac{\sigma_0}{E} \qquad (2)$$

where

P' is load per unit length, N/cm
P is load on a sphere, N
E is the modulus of elasticity of the half space, N/cm2
v is the Poisson's ratio, taken as 0.35.

Similarly, the contact of a spherical body on the plane surface gives the following expressions:

$$r = 0.87 \cdot \left(\frac{P \cdot R}{E} \right)^{1/3} \qquad (3)$$

$$z = 0.7566 \cdot \left(\frac{P^2}{R \cdot E^2} \right)^{1/3}$$

$$\sigma_0 = 0.63 \cdot \left(\frac{P \cdot E^2}{R^2} \right)^{1/3} \qquad \text{and} \qquad \frac{z}{r} = 1.38 \cdot \frac{\sigma_0}{E} \qquad (4)$$

where

P is load on a sphere, N

Comparison of Eqs. (2) and (4) suggests that, for the same maximum stress, a spherical body has a larger deformation than a cylindrical body.

The pressure distribution in the half space under the contact surface is shown in Figure 3. Under a spherical body the decrease of normal stresses occurs more rapidly compared to those of a cylindrical body as a function of the relative depth. Due to the relative coordinate (*z/b*, *z/r*), the absolute value of deformations increases in the same ratio as the radius or half width of the loaded surface. Using a coarser grit size and the same overall surface pressure, the same stress level occurs deeper under the loaded surface and, therefore, the crushing effect of the vertical stress will be larger. It should be here noted that crushing effect of the vertical stress will considerably enhanced by shear stresses appearing due to the horizontal motion of the working edges.

Keeping in mind the stress distribution in Fig. 3 it is obvious that a bigger radius of a sphere is equivalent to smaller radius for cylindrical edges concerning their effect on the Rk-layer thickness.

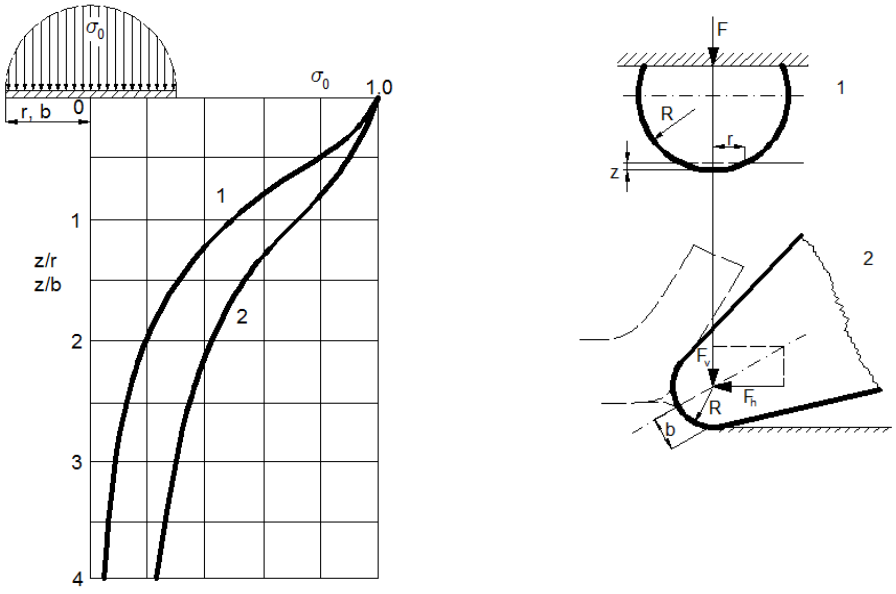

Figure 3. Stress relations under a spherical (1) and cylindrical body (2) using hemispherical pressure distribution in the contact surface

It is interesting to examine the maximum stress under grit as a function of grit size supposing the same grit cover ratio.

Taking 1 cm^2 surface area, the number of particles depends on the particle diameter and the cover ratio:

$$n \cdot \frac{d_i^2 \cdot \pi}{4} = 1.0 \cdot \Psi \qquad \text{and} \qquad n = \frac{1.273 \cdot \Psi}{d_i^2}$$

where:

d_i is the particle diameter, cm;

Ψ is the particle cover ratio on the surface.

Exerting a p pressure onto the surface (N/cm^2), the force acting on a single particle is calculated as

$$P_i = \frac{p}{n} = \frac{p \cdot d_i^2}{1.273 \cdot \Psi} \tag{5}$$

The radius of deformation is given by the known Boussinesq equation and making use of the previous equation:

$$r = \left(\frac{3}{4} \cdot P \cdot R \frac{\left(1 - \nu^2\right)}{E} \right)^{1/3} = 0.637 \cdot d_i \cdot \left(\frac{p}{\Psi \cdot E} \right)^{1/3} \tag{6}$$

and the maximum contact pressure under the grit is

$$\sigma_0 = 0.923 \cdot \left(\frac{p}{\Psi} \right)^{1/3} \cdot E^{2/3} \quad \text{[N/cm}^2\text{]} \tag{7}$$

where: E is the modulus of elasticity of the wood material, N/cm^2.

Eq. (7) clearly shows that the maximum stress under the grit does not depend on the grit size.

It should be noted that the above considerations and calculations refer to solid body without cavities. Therefore, depending on the internal structure of wood, much higher local stresses may be expected which will be capable of doing ruptures in the material. Due to the horizontal moving of the edge, a shear stress field will be superimposed which further enhances the destroying effect of the vertical stress field.

For a given case, the stress decay as a function of depth can easily be calculated. As an example and for comparison, Fig. 4 shows the rapid decrease of stresses under the surface for two sandpaper grades. It is clearly seen that the coarser grit exerts a given stress roughly two times deeper than finer grit. As a consequence, the crushing effect which follows a given stress level also effects a deeper zone increasing the R_k-layer considerably.

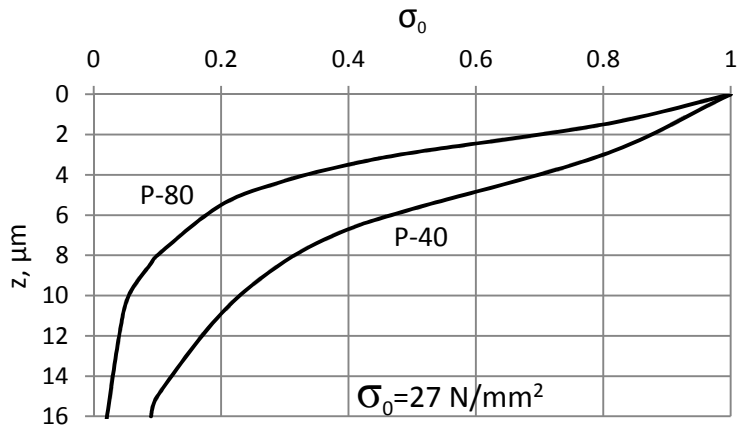

Figure 4 Stress decay under a grit as a function of depth.

$E = 1400\ \text{N/mm}^2,\ p = 1\ \text{N/cm}^2,\ \Psi = 0.8$

Materials and methods

In this study five different wood species (spruce, larch, beech, black locust and oak) were selected to carry out the experimental work. Three 20 x 5 x 1.5 cm samples were cut tangentially from each wood species. They were subjected to sanding using a belt sander. The sanding velocity was 24.6 m/s with surface pressure between 0.25 – 0.35 N/cm^2. Four grit sizes were selected: Korund P-80, P-120, P-150 and P-240. The samples were sanded lengthwise while roughness measurements were taken crosswise. Ten repeated measurements were made on each sample to ensure reliable results.

For the measurement of roughness a MAHR stylus unit (Model S2, PZK MFW 250) was used. The pick-up has a skid type diamond stylus with a tip radius of 5 µm. The active tracing length is 12.5 mm. Each measurement was represented by surface profile, the Abbott-curve and the calculated standard roughness parameters.

The samples came from the same boards used in earlier experiments when the anatomical properties were determined. These properties were used to calculate the structure number *ΔF* (Table 1) [6].

Table 1 Structural properties of specimens

wood species	early wood			late wood		
	$\overline{d_i}$ [µm]	$\overline{n_i}$ [piece/cm^2]	$\overline{a}$	$\overline{d_i}$ [µm]	$\overline{n_i}$ [piece/cm^2]	$\overline{b}$
spruce	30.0	111 335	0.8478	19.0	160 400	0.1522
pine	28.0	125 100	0.6694	20.0	135 840	0.3306
larch	38.0	65 490	0.6310	17.5	145 000	0.3690

beech (vessel)	66.0	15 740	0.7000	48.0	14 020	0.3000
beech (tracheid)	8.2	342 890		6.4	490 290	
b. locust (vessel)	230.0	546	0.5800	120.4	1 500	0.4200
b. locust (tracheid)	15.0	270 000		9.6	280 000	
oak (vessel)	260.0	400	0.5900	35.7	12 000	0.4100
oak (tracheid)	22.5	120 000		19.6	85 000	

Notations in Table 1: $\overline{d_i}$ is the average diameter of vessels and tracheids, $\overline{n_i}$is the average number of vessels and tracheids in the unit cross-section, $\bar{a}$ is the average portion of early wood, $\bar{b}$ is the average portion of late wood.

Experimental results

The processing method of recent experimental results substantially follows that of earlier experiments related to machined surfaces [1, 5, 6]. New interrelations and a material characterization method have been discovered and introduced for better understanding the origin of surface roughness and its relations to the internal structure of different wood species.

The average roughness R_a has also correlation with the irregularity depth R_z which is depicted in Fig. 5 using all grit sizes and wood species tested. A similar relationship is found also for planed surfaces. These interrelations facilitate a quick estimation of one parameter from an other.

The average roughness R_a as a function of the sum (R_{pk}+R_k+R_{vk}) shows a quite similar picture compared to the machined surface (Figure 6) [5]. However, a fine sanding (P-240) results in a somewhat lower average roughness. The curve for machined surface coincides with the curve for P-80. The curves are valid for all wood species tested.

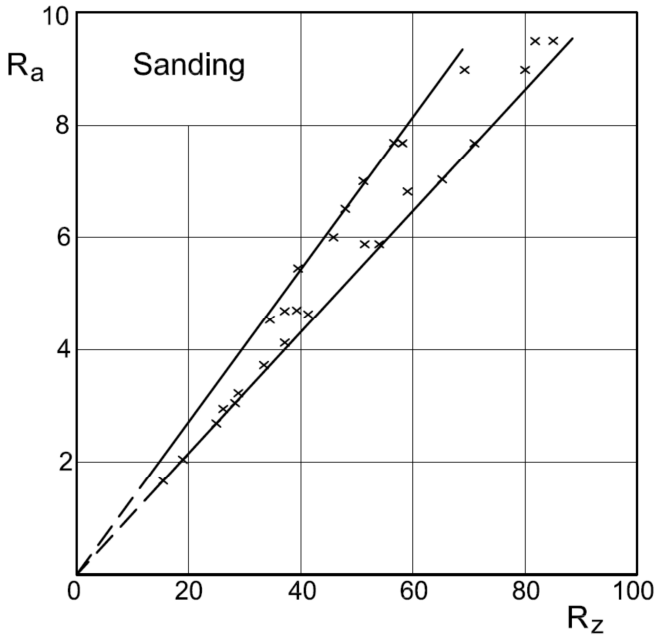

Figure 5 Relationship between R_a and R_z at sanding for different wood species.

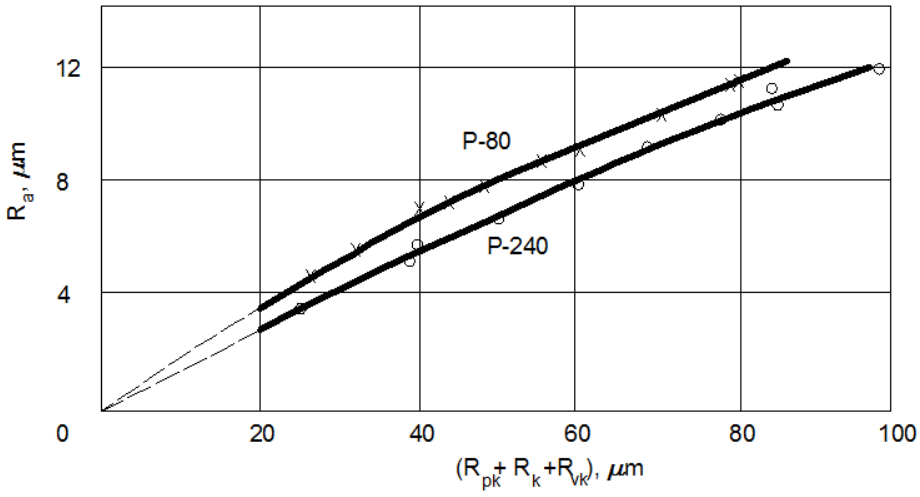

Figure 6 The average roughness R_a as function of the sum (R_{pk}+R_k+R_{vk})

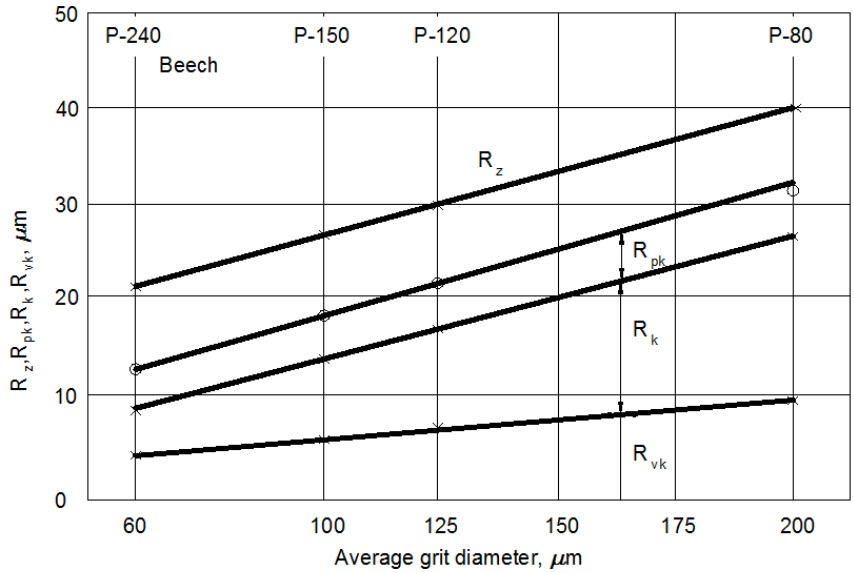

Figure 7 Effects of grit size on the surface roughness parameters for beech wood

A detailed roughness representation for beech wood is given in Figure 7 as a function of average grit size diameter. The relationship is almost linear for all roughness components. The strong dependence of the R_k-layer is striking. This finding refers to the strong influence of the particle diameter on the crushing depth in the surface layer.

An even stronger dependence of the R_k layer can be observed in Fig. 8 representing the measurement results for larch wood. In this case the components show a slight diviation from the linear variation as a function of grit size diameter.

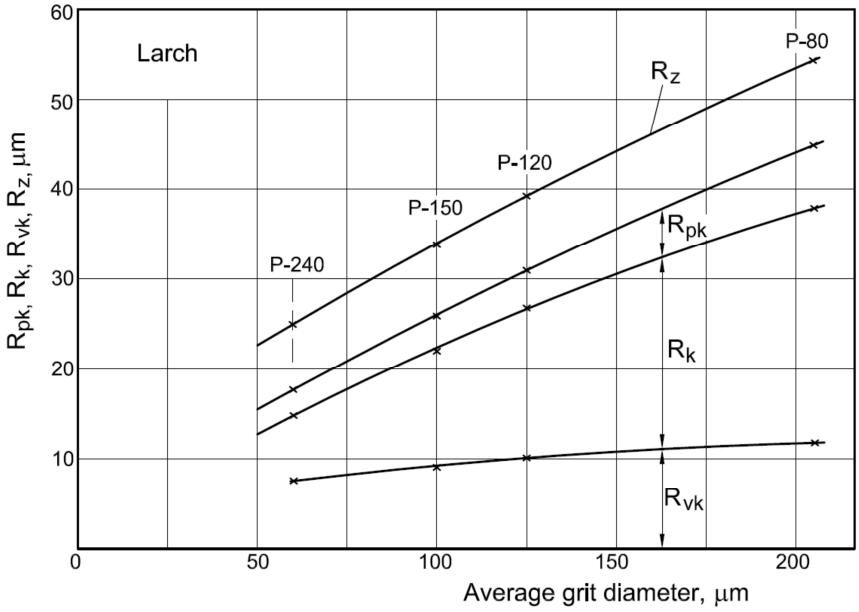

Figure 8 Relationship between grit size and roughness parameters for Larch with density of 700 kg/m^3

The smoothness of a surface is considerably determined by the reduced peak heights. This relationship for spruce and beech is given in Figure 9 on double logarithmic scale. The decrease of grit size allows achieving quite low values which would give a good polishing possibility using wax or light-colored oils. The polishing ability of a surface plays a definite role in the colour enhance of a given wood species [7].

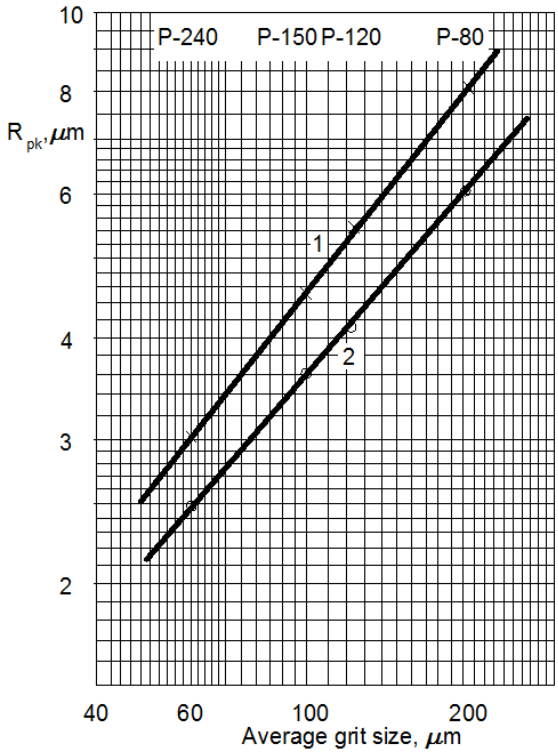

Figure 9 Relationship between the reduced peak heights R_{pk} and grit size
1 – Spruce, 2 – Beech

As mentioned before (see Fig. 3 and 4), the core depth R_k should have a strong correlation with the grit size. Figure 10 shoes the R_k/R_z-ratio as a function of structure number ΔF. Again, the relationship is quiet similar to those of machined surfaces and the P-240 curve almost coincides with the curve valid for machined surfaced. Here we can make an interesting comparison: the average edge radius for knives in the working-sharp condition is 20 µm, while the average grit radius for P-240 is 30 µm. This experimental result is in full agreement with Figure 3 due to the different action of sphere and cylinder on the half space.

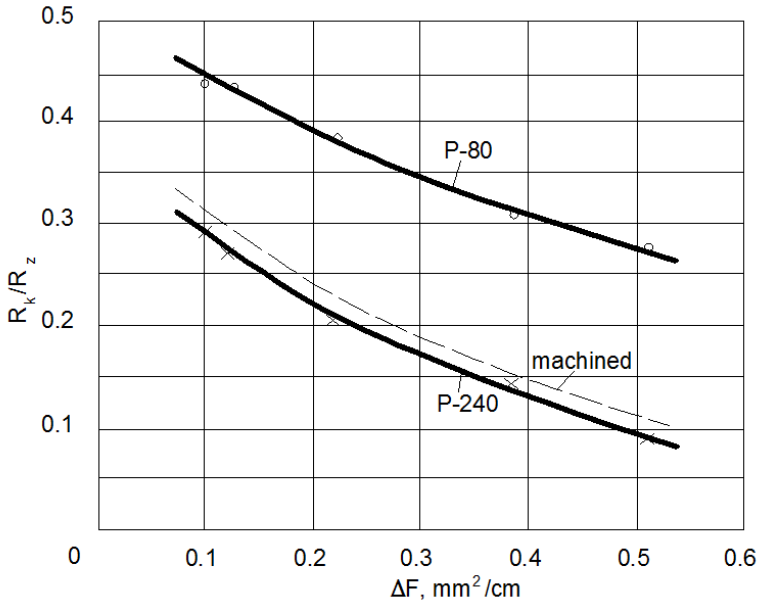

Figure 10 Relative core depth as a function of structure number *ΔF*

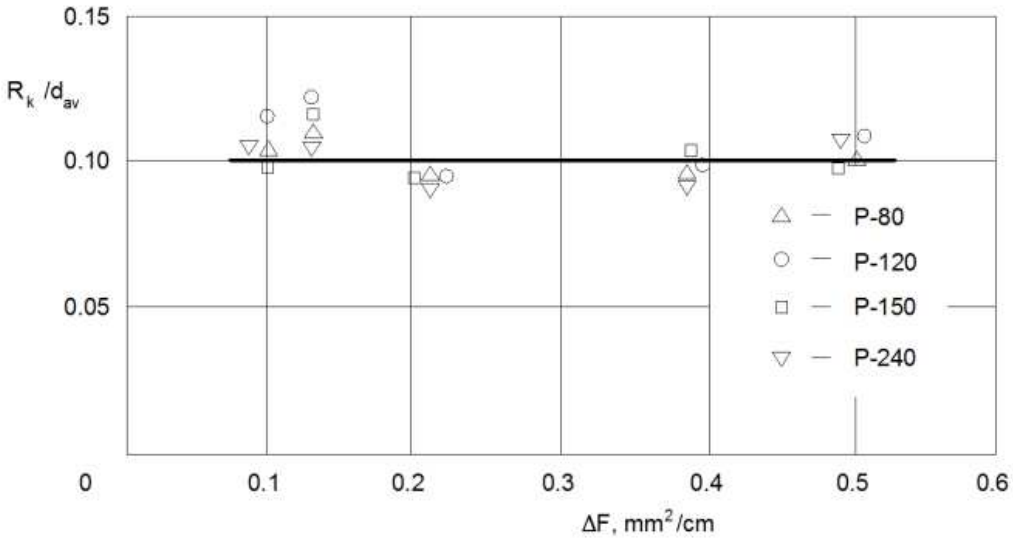

Figure 11 Core depth and grit diameter ratio depending on the structure number *ΔF*

An other interesting finding that the core depth R_k related to the average grit diameter is constant for all wood species. This relationship is shown in Figure 11 which gives a possibility to forecast the expected R_k-layer in advance or to select an appropriate grit size to achieve a given R_k-layer thickness.

Several roughness parameter ratios can be constituted uniquely depending on the structure number *ΔF*. The results illustrated in the following Figure refer to milled and sanded surfaces. The results due to sanding are mainly valid for sandpaper grades between P80 and P150.

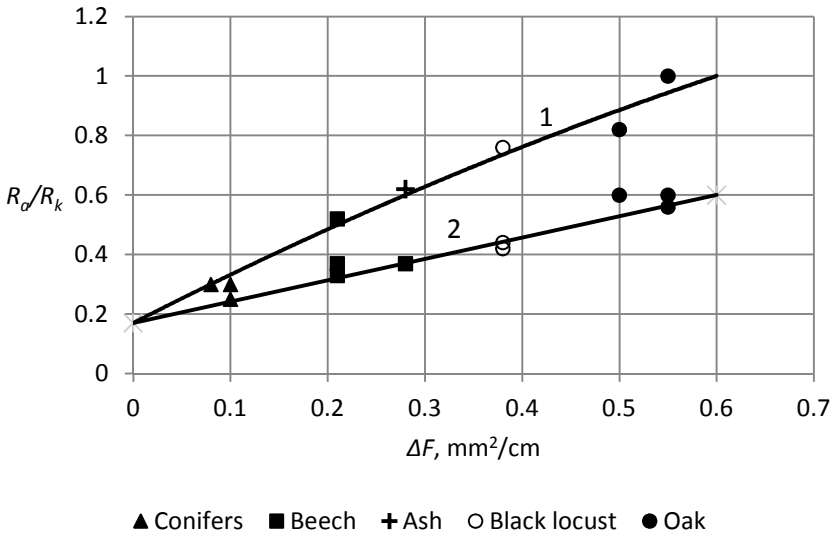

Figure 12 Variation of R_a/R_k ratio as a function of structure number. 1 – milled, 2 – sanded

Fig. 12 represents the R_a/R_k ratio for milled and sanded surfaces as a function of structure number. This ratio shows the relative contribution of the R_k layer to the average roughness. Conifers lacking deep valleys have a stronger dependence on the R_k layer thickness. The sanding of the surface restructures the height distribution and increases the role of the R_k layer, especially at hard wood species.

The reduced valley depth R_{vk} related to the R_z-value shows also a strong correlation with the average grit diameter. Figure 13 demonstrates this relationship for the wood species tested. The spruce, larch and beech have similar values, while black locust and oak show significantly higher R_{vk}-values.

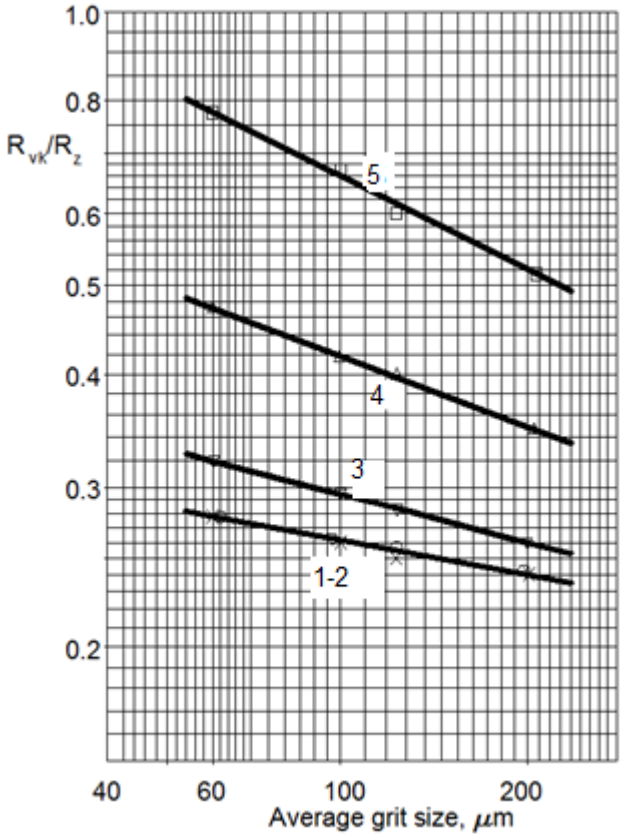

Figure 13 The R_{vk}/R_z ratio as a function of grit size
1 – Spruce, 2 – Beech, 3 – Larch, 4 – Black Locust 5 - Oak

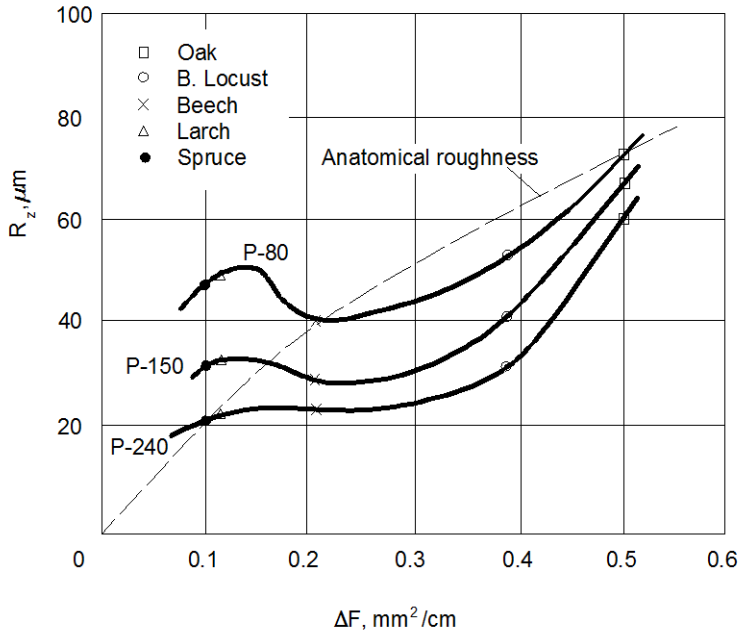

Figure 14 An overview of R_z-values for all wood species as a function of structure number ΔF

An overall view on the irregularity depth R_z for all wood species is given in Figure 14, showing also the anatomical minimum roughness.

Measurement results have clearly shown that the average roughness R_z may be considerably less than the anatomical roughness [5, 6] for a given wood species. This is possible only in the case, if the surface layer undergoes a structural change due to cell deformation. Besides the crushing effect of the spherical edges, a clogging effect (compression) takes place decreasing the cavities in number and size which do appear in the roughness measurement result.

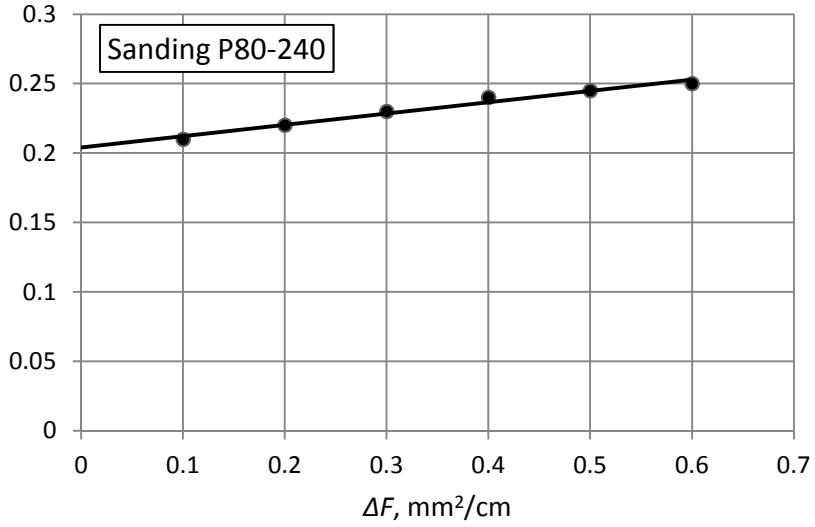

Figure 15 Dimensionless plot of experimental results of sanding using different sanding grades and wood species

The processing of a vast amount of experimental results has revealed that the following dimensionless number $R_a / \sqrt{R_k \cdot R_z}$ is more or less constant (invariant) independently of machining operations and wood species.

The averaged measurement data for sanding using grit grades between P-80 and 240 are represented in Fig. 15 as a function of structure number *ΔF*. The dimensionless number is slightly increasing toward big vessel species; however, the variation is not very large. As a first approximation, the dimensionless number may be regarded as constant with a value of 0.23. This finding highly facilitates the generalization of experimental results and evaluation of the sanding process.

It is important to notice that the local compression of the material under the working edge depends on the local strength and not on the overall strength of the material. The local strength of wood materials today is not known, but estimation for comparison is possible using the structural properties of the wood materials in question. These structural properties are given in Table 1.

The beech seems to be very sensitive to the compression effect of the edge. Looking at the structural properties, we can see the very large number of tracheids both in the early and late wood. A large number of cavities in a given cross-section mean thinner cell walls which can be deformed and compressed easier decreasing the bigger cavities. As a consequence a clogging effect due to surface layer deformation occurs.

Comparing the black locust and oak, we can see a similar case: the number of tracheids of black locust in the early and late wood surpasses those of the oak twice to threefold. Therefore, the oak will be clogged much less than the black locust, in spite of the fact, that the structure numbers of black locust and oak are not far from one another. As a consequence, the black locust shows a much smoother surface compared to the oak for the same sanding.

Conclusions

Based on the theoretical considerations and experimental results, the following main conclusions may be drawn

- between the standard grit size *P* and the average grit diameter a hyperbolic relationship exists,
- the stress under a grit, as a spherical edge, is depending on the surface pressure and the modulus of elasticity of the wood material, but does not depend on the grit size,
- it is proved theoretically and experimentally that the core depth R_k strongly depends on the average grit diameter used,
- experimental results show that all three components of the Abbott-curve (R_{pk}, R_k, R_{vk}) are nearly linear increasing with greater grit diameters,
- an interesting finding that the R_k/d_{av} ratio remains constant for all wood species tested
- related roughness parameters (R_k/R_z, R_{vk}/R_z) show definite relationships as a function of either the structure number ΔF or the average grit diameter,
- experimental results show that the roughness after sanding may be smaller than the anatomical roughness of the given wood species. This may happen only as a consequence of clogging due to surface deformation by the grits.

References

1. Csanády, E. and E. Magoss, Mechanics of Wood Machining. Springer Verlag, Berlin, 2012
2. Westkamper, E. und A. Riegel, Qualitatskriterien für geschliffene Massivholzoberfachen. Holz als Roh- und Werkstoff, 1993, S.123-125.
3. Scholz, F. and J. Ratmasingam, Optimization of sanding process. Proc. of 17th IWMS Rosenheim, 2005, pp. 422-429.
4. Siklinka, M. and A. Ockajova, The study of selected parameters in wood sanding. Proceedings of 15th IWMS Los Angeles, 2001, pp. 485-490.
5. Magoss, E. and G. Sitkei, Fundamental relationships of wood surface roughness at milling operations. Proc. of 15th IWMS Los Angeles, 2001, pp. 437-446.
6. Magoss, E. und G. Sitkei, Strukturbedingte Rauheit von mechanisch bearbeiteten Holzoberfächen. Möbeltage in Dresden, 2000, Tagungsbericht S. 231-239.